

## Application of Phase Contrast Transmission Microscopic Methods to Polymer Materials

Masatoshi Tosaka\*

*Institute for Chemical Research, Kyoto University, Gokasyo, Uji, Kyoto-fu 611-0011, Japan*

Radostin Danev and Kuniaki Nagayama

*Okazaki Institute for Integrative Bioscience, National Institutes of Natural Sciences, 5-1, Higashiyama, Myodaiji-cho, Okazaki, Aichi-ken 444-8787, Japan*

Received June 9, 2005

Revised Manuscript Received August 4, 2005

**Introduction.** Transmission electron microscopy (TEM) is a common method for structural studies on polymers. Among variety types of microscopic methods, TEM is advantageous in terms of the high spatial resolution, capability to analyze internal structure of specimens, and so on.

In the customary TEM observation, there is a potential problem that usual polymer samples themselves do not present enough contrast in their images. This is because they are composed of light elements having only weak scattering power for electrons; polymer samples are basically “transparent” for the observation by conventional TEM (C-TEM). Therefore, the preparation process of most amorphous specimens for TEM must include a step that deposits heavy metal atoms on specific locations of the samples by, e.g., the electron staining or the metal shadowing techniques.<sup>1,2</sup> As the strongly scattered electrons by the heavy metal atoms are cut off due to the finite aperture size in the objective plane, the locations of the metal atoms appear darker in the TEM images, contrasted with the bright surroundings. With these techniques, a variety of systems have been successfully studied so far.

However, there are a lot of samples that are not suitable for the metal-depositing techniques. Some polymer samples cannot be stained at all, and some others are entirely stained, both leading to useless images showing no structural features. The metal-depositing techniques are not suitable also for in situ observation of structural changes. For observation of such specimens by C-TEM, strong defocusing is necessary.<sup>1,3–8</sup> Otherwise, we must use very small objective aperture<sup>1</sup> to give rise to recognizable contrast. Both observation conditions in turn permit merely low resolution.

In the case of optical observation, phase contrast optical microscopy (PCOM) and differential interference contrast optical microscopy have been widely used for such “transparent” specimens. PCOM uses a Zernike phase plate to provide phase contrast. Though the principle of PCOM is applicable to TEM, the Zernike phase contrast method has not been put into practice for TEM due to technical problems. Recently, however, such problems were overcome, and two methods for phase contrast TEM (PC-TEM) were put into practical use. The details of the instruments and the principles of the PC-TEM have been described elsewhere.<sup>9,10</sup> In this communication, we present examples of PC-TEM

observation and demonstrate potential advantages of the method.

**Experimental Section.** The transmission electron microscope used in this study was a JEM-3100FFC by JEOL Ltd., which is equipped with a field emission gun, a cryogenic specimen stage cooled with liquid helium, an energy filter, and CCD cameras. The objective lens was specially designed to accommodate the phase plates accurately on the back focal plane. Two types of phase plates can be freely inserted into and removed from the optical path, and accordingly, we can switch the instrument among the two phase contrast modes and the conventional one. The accelerating voltage was 300 kV. All the images presented in this paper were taken at 4.2 K using the energy filter (zero loss) and recorded as digital data (2 byte, 2048 × 2048 pixel) by the CCD camera. (The brightness and contrast of the pictures in this paper have been automatically adjusted to be displayed with maximum contrast for each image before trimming.)

The natural rubber sample filled with carbon black (NR-CB) was prepared in a similar way as in ref 11. In this case, 10 parts of carbon black, 2 parts of stearic acid, 1 part of active zinc oxide, 1 part of *N*-cyclohexyl-2-benzothiazole sulfenamide, and 1.5 parts of sulfur were used for 100 parts of rubber. Thin sections of the NR-CB sample were prepared by using a cryo-ultramicrotome. Thin sections of block copolymer of polystyrene and polyisoprene (PS-*b*-PI) were kindly supplied from Prof. H. Hasegawa, Graduate School of Engineering, Kyoto University. The molecular weight of the polystyrene segment was  $48.9 \times 10^3$  g/mol, and that of polyisoprene segment was  $46.8 \times 10^3$  g/mol.

**Results and Discussion.** Parts a–c of Figure 1 show the TEM images of NR-CB at the same location. The C-TEM images in parts a and b were taken without the phase plates and the objective aperture. Though carbon black particles are dimly recognized in the C-TEM image (Figure 1a), the contrast is not enough to discuss the structural details. By defocusing strongly, the contrast of C-TEM images can be improved, as shown in Figure 1b. In this case, however, small structures are not resolved. Figure 1c is the Zernike phase contrast TEM (ZPC-TEM) image using a Zernike phase plate made of a thin carbon film with a small hole in the center.<sup>9</sup> The phase of the scattered beams is shifted by the carbon film, while the unscattered beams pass through the center hole without the phase shift. At the image plane, the unscattered and scattered beams are combined, and the interference between them provides strong phase contrast.<sup>9</sup> Thus, the contrast of the ZPC-TEM image is drastically improved without losing the information on structural details.

The ZPC-TEM image in Figure 2 was taken from a different part of the NR-CB sample. In this figure, the (001) lattice fringes (which correspond to 4.37 nm according to the reported lattice constant<sup>12</sup>) of stearic acid crystals are observed together with the carbon black particles. It is noted that the samples with rubber matrix are usually not suitable for electron staining because the heavy metal atoms are deposited in the matrix phase and the entire sample becomes dark. Such clear images of the rubber–carbon black system recording the structural details as in Figures 1c and 2 could

\* Corresponding author: e-mail: [tosaka@scl.kyoto-u.ac.jp](mailto:tosaka@scl.kyoto-u.ac.jp); Tel +81-774-38-3062; Fax +81-774-38-3067.

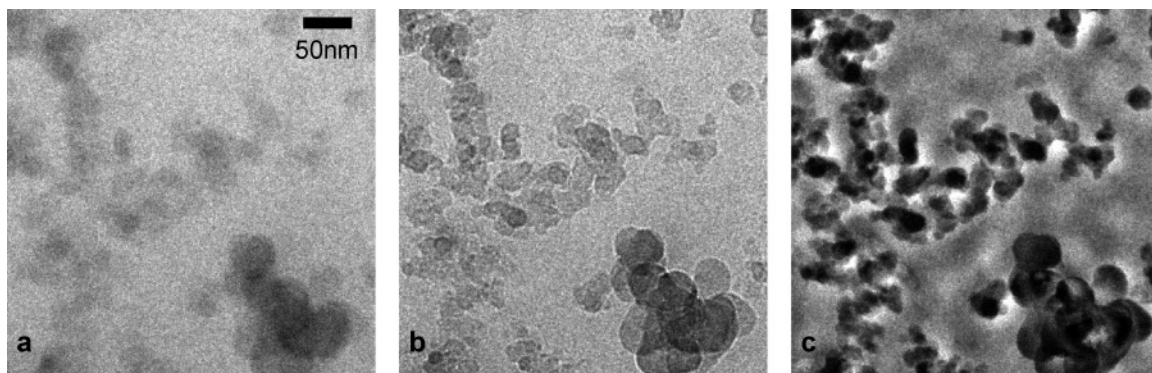


**Figure 1.** TEM images of the NR-CB sample taken at a setting magnification of 20 000: (a) C-TEM image near the just focus; (b) C-TEM image at 10  $\mu\text{m}$  underfocus; (c) ZPC-TEM image near the just focus.

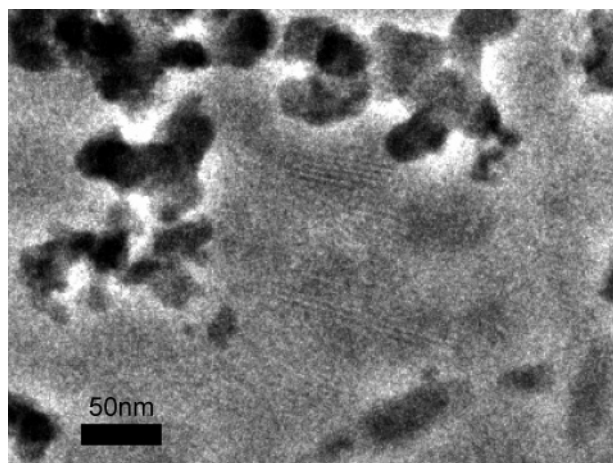


**Figure 2.** ZPC-TEM image of the NR-CB sample taken at a setting magnification of 20 000. The carbon black particles and the (001) lattice fringes of stearic acid crystals are clearly observed together.

be taken for the first time by ZPC-TEM. The ability to provide high contrast for both small (less than 1 nm) and large structures of unstained specimens is the important feature of the PC-TEM.<sup>9</sup>

By using a semicircular phase plate, another type of PC-TEM, namely the Hilbert differential contrast TEM (HDC-TEM), can be implemented.<sup>10</sup> HDC-TEM images have quasi-topographic contrast, which is not directly related to the 3-dimensional shape of the object. Figure 3a shows an example of the HDC-TEM image. The HDC-TEM image also maintains the information on the detailed structure. For example, the (001) lattice fringes of the stearic acid crystals are observed also in the HDC-TEM image (Figure 3b). The HDC-TEM image is more perceptible due to the quasi-topographic contrast. On the other hand, the interpretation of the HDC-TEM images may be difficult in some cases. However, if an HDC-TEM image is quantitatively recorded together with the corresponding C-TEM image, by adopting an appropriate image-processing procedure, reconstruction of a new image composed of the phase component is possible, which appears like the ZPC-TEM image.<sup>13</sup> As HDC-TEM can recover low spatial frequency (namely, the larger spacing) with higher contrast than ZPC-TEM,<sup>10</sup> the former is more convenient for the observation of global structures such as the phase separation structures.

Figure 4a shows the HDC-TEM image of unstained PS-*b*-PI. The lamellar structure as a result of phase separation is clearly seen. A C-TEM image of the stained

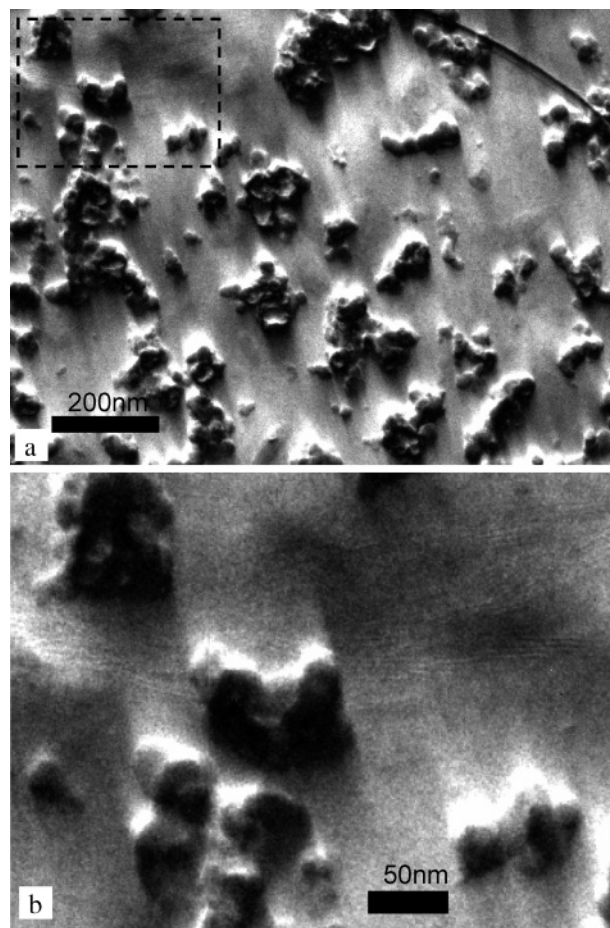


**Figure 3.** HDC-TEM image of the NR-CB sample taken at a setting magnification of 20 000. (a) Quasi-topographic image was obtained. (b) Enlargement of the rectangular part of (a) indicated by the broken lines. The carbon black particles and the (001) lattice fringes of stearic acid crystals running horizontally are observed together, also in this image.

sample using  $\text{OsO}_4$  is shown in Figure 4b for comparison. The unstained PS-*b*-PI did not present perceptible contrast when the sample was observed by C-TEM near the just focus, though we could dimly observe the same lamellar structure as in Figure 4a by defocusing strongly ( $\sim 70 \mu\text{m}$ ).<sup>3,14,15</sup> The periodicity of the lamellar structure is slightly different between parts a and b of this figure, which should be due to local fluctuation of the phase separation structure. The same periodicity as in Figure 4b has been observed by HDC-TEM for the unstained sample at another location. Though we cannot attribute the dark and bright part to the polystyrene



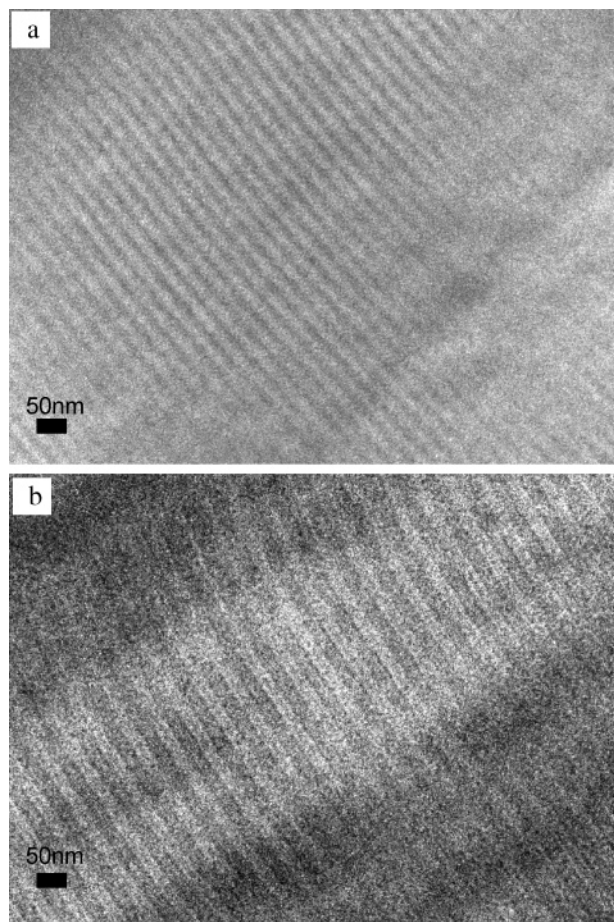


**Figure 4.** TEM images of the PS-*b*-PI samples taken at a setting magnification of 15 000: (a) HDC-TEM image of the unstained sample; (b) C-TEM image of the sample stained by OsO<sub>4</sub> for 1 h at room temperature.

and polyisoprene phases only from the HDC-TEM image, a study using a series of samples with different block composition would enable to do so.

In this way, by PC-TEM, we can observe unstained polymer samples without significant loss of resolution. It is true that there are other techniques to visualize the structural details without electron staining. For example, the conventional dark-field imaging will highlight crystalline regions. The element mapping techniques<sup>16</sup> or the annular dark-field techniques in combination with the scanning TEM<sup>17</sup> will visualize distribution of specific elements. However, these techniques utilize only a part of the incident electron energy and require more irradiation than usual bright-field observation. Accordingly, the problem of the radiation damage arises for many of the polymer samples. Low-voltage

electron microscopy<sup>18</sup> is another candidate to observe unstained polymer samples. However, the low-voltage electrons result in the severer radiation damage, and the electron beams can penetrate only thin (<50 nm) samples. As the illumination condition for PC-TEM is almost the same as the conventional bright-field TEM, the radiation damage does not increase, and the same specimens as C-TEM can be observed.

We have already studied other samples with PC-TEM and found some structures which have not been recognized. They will be reported separately in the near future.

**Acknowledgment.** The authors are grateful to Prof. H. Hasegawa for providing us with the sample of PS-*b*-PI. This research is partially supported by the Ministry of Education, Science, Sports and Culture, Grant-in-Aid for Creative Scientific Research, 13GS0016 (2001–2006).

## References and Notes

- (1) Tsuji, M. In *Comprehensive Polymer Science*; Booth, C., Price, C., Eds.; Pergamon Press: Oxford, 1989; Vol. 1, pp 785–840.
- (2) Tsuji, M.; Fujita, M. In *The Encyclopedia of Materials: Science and Technology*; Buschow, K. H. J., Cahn, R. W., Flemings, M. C., Ilshner, B., Kramer, E. J., Mahajan, S., Eds.; Elsevier Sci.: Amsterdam, 2001; pp 7654–7664.
- (3) Martin, D. C.; Thomas, E. L. *Polymer* **1995**, *36*, 1743–1759.
- (4) Tsuji, M.; Shimizu, T.; Kohjiya, S. *Polym. J.* **1999**, *31*, 784–789.
- (5) Tsuji, M.; Shimizu, T.; Kohjiya, S. *Polym. J.* **2000**, *32*, 505–512.
- (6) Shimizu, T.; Tosaka, M.; Tsuji, M.; Kohjiya, S. *Rubber Chem. Technol.* **2000**, *73*, 926–936.
- (7) Shimizu, T.; Tsuji, M.; Kohjiya, S. *Sen'i Gakkaishi* **2001**, *57*, 137–143.
- (8) Shimizu, T.; Tsuji, M.; Kohjiya, S. *J. Mater. Res.* **1999**, *14*, 1645–1652.
- (9) Danev, R.; Nagayama, K. *Ultramicroscopy* **2001**, *88*, 243–252.
- (10) Danev, R.; Okawara, H.; Usuda, N.; Kametani, K.; Nagayama, K. *J. Biol. Phys.* **2002**, *28*, 627–635.
- (11) Poompradub, S.; Tosaka, M.; Kohjiya, S.; Ikeda, Y.; Toki, S.; Sics, I.; Hsiao, B. S. *J. Appl. Phys.* **2005**, *97*, 103529/1–103529/9.
- (12) Müller, A. *Proc. R. Soc. London* **1927**, *114A*, 542–561.
- (13) Danev, R.; Nagayama, K. *J. Phys. Soc. Jpn.* **2004**, *73*, 2718–2724.
- (14) Handlin, Jr., D. L.; Thomas, E. L. *Macromolecules* **1983**, *16*, 1514–1525.
- (15) Handlin, Jr., D. L.; Thomas, E. L. *J. Mater. Sci., Lett.* **1984**, *3*, 137–140.
- (16) Ribbe, A. E.; Okumura, A.; Matsushige, K.; Hashimoto, T. *Macromolecules* **2001**, *34*, 8239–8245.
- (17) Taubert, A.; Winey, K. I. *Macromolecules* **2002**, *35*, 7419–7426.
- (18) Drummy, L. F.; Yang, J.; Martin, D. C. *Ultramicroscopy* **2004**, *99*, 247–256.

MA0512197